

Non-resonant parametric amplification in biomimetic hair flow sensors: Selective gain and tunable filtering

H. Droogendijk,^{a)} C. M. Bruinink, R. G. P. Sanders, and G. J. M. Krijnen
 MESA⁺ Institute for Nanotechnology, University of Twente, Enschede, The Netherlands

(Received 14 September 2011; accepted 31 October 2011; published online 21 November 2011)

We demonstrate that the responsivity of flow sensors for harmonic flows can be improved significantly by non-resonant parametric amplification. Using electrostatic spring softening by AC-bias voltages, increased responsivity and sharp filtering are achieved in our biomimetic flow sensors. Tunable filtering is obtained for non-resonant electromechanical parametric amplification, applicable at a wide range of non-resonant frequencies while achieving highly selective gain of up to 20 dB. © 2011 American Institute of Physics. [doi:10.1063/1.3663865]

Nature displays a variety of mechanisms that constitute exceptional sensory performance, e.g., with respect to sensitivity, dynamic range, frequency filtering, and selectivity,¹ which form a rich source of inspiration to engineers. Inspired by crickets and their perception of flow phenomena, artificial hair flow sensors have been developed in our group.² Improvement of fabrication methodologies (Fig. 1) has led to better performance, making it possible to detect flow velocities in the sub-mm/s range.³ To further improve the performance of these sensors and implement adaptive filtering, we make use of non-resonant parametric amplification (PA). By modulating the torsional stiffness of the sensory system, we can make it selective for arbitrary flow frequencies and simultaneously achieve significant amplification of the sensor response.

Parametric amplification exploits complex interactions between excitatory signals in which amplitude, frequency, and phase play important roles in the entanglement of the signals determining the overall response. Previous research^{4,5} shows a system operating at resonance and, with proper choices of parameters, exhibiting amplification of the input of the system. In contrast, in this work, we do not operate at the sensor's resonance but still achieve electro-mechanical filtering and selective gain.

The motion of a flow susceptible hair is described by a second order mechanical system,⁶ wherein a hair is driven to periodic rotations by a drag torque with amplitude T_0 and angular frequency ω_a , caused by viscous forces⁷ associated with a harmonic air flow. The system's response in terms of its hair rotational angle θ is governed by its moment of inertia J , torsional resistance R , and torsional stiffness S ,

$$J \frac{d^2\theta(t)}{dt^2} + R \frac{d\theta(t)}{dt} + S(t)\theta(t) = T_0 \cos(\omega_a t). \quad (1)$$

To exploit parametric amplification in the hair-based flow sensor, an AC-bias voltage is symmetrically supplied to the electrodes, inducing balanced electrostatic forces (Fig. 2). As a result, the torsional stiffness S is modulated giving $S(t)$.

The resulting time-dependent stiffness $S(t)$ is calculated from the geometry of the rotating parallel plate capacitor

with width w , total length $2L$, and mutual plate distance g . The sensor operates in air, for which the relative electric permittivity ϵ_r is assumed to be equal to 1. Additionally, the silicon-nitride layers add some dielectric distance to the gap given by $t_{\text{SiN}}/\epsilon_{r,\text{SiN}}$, leading to an effective gap g_{eff} ,

$$g_{\text{eff}} = \frac{t_{\text{SiN,top}}}{\epsilon_{r,\text{SiN}}} + g + \frac{t_{\text{SiN,bottom}}}{\epsilon_{r,\text{SiN}}}. \quad (2)$$

Using the parallel plate approximation, the angle dependent capacitance $C(\theta)$ is given by

$$C(\theta) = \epsilon_0 w \frac{\cos(\theta)}{\sin(\theta)} \ln \left(\frac{g_{\text{eff}} + L \sin(\theta)}{g_{\text{eff}} - L \sin(\theta)} \right), \quad (3)$$

where θ is the angle of rotation of the upper plate. Applying transduction principles, the electrostatically softened torsional stiffness $S(t)$ on application of an AC-bias voltage with amplitude U_p , angular frequency ω_p , and phase ϕ_p is given by

$$S(t) = S_0 - \frac{1}{4} U_p^2 \frac{\partial^2 C}{\partial \theta^2} - \frac{1}{4} U_p^2 \cos(2\omega_p t + 2\phi_p) \frac{\partial^2 C}{\partial \theta^2}. \quad (4)$$

As a result, the torsional stiffness $S(t)$ is dependent on frequency, phase, and amplitude of the applied AC-bias voltage, further referred to as pump signal. Under the small

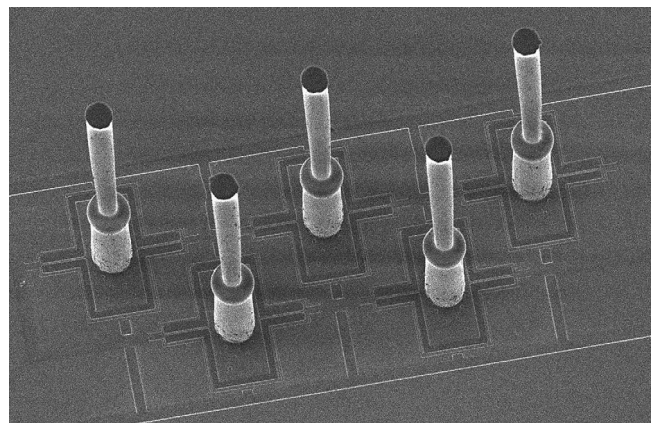


FIG. 1. MEMS hair flow sensors fabricated by surface micromachining and using SU-8 lithography.

^{a)}Electronic mail: h.droogendijk@utwente.nl.

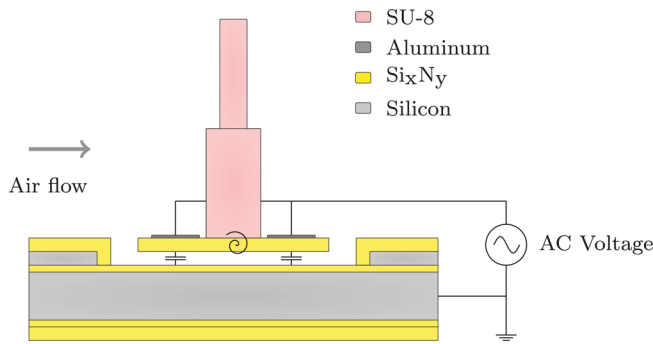


FIG. 2. (Color online) Modulating the torsional stiffness in time by applying AC-bias voltages to the sensor's capacitances.

rotational angles normally encountered, the total torsional stiffness $S(t)$ contains the intrinsic material-based stiffness S_0 , a time-independent softening term, and a frequency and phase-dependent softening term.

For specific conditions, the solution of Eq. (1) can be obtained using analytical methods and approximations.⁸ However, as a more general approach to modeling our electromechanical system, allowing investigation of non-resonant interactions, a strong pump and a low quality factor (our flow sensors are nearly critically damped systems), numerical simulations are used to determine the system behavior. Using the ode4 explicit fixed-step solver from Simulink shows that significant amplification is achieved when periodic softening occurs at twice the flow frequency f_a of the system, requiring frequency matching of the pump to the harmonic air flow ($f_a = f_p$).

To study the system performance and to determine its selectivity, the analysis is divided into two areas: matching the frequencies of flow and pump ($f_p = f_a$) and non-matching of these frequencies ($f_p \neq f_a$). Furthermore, the pump phase ϕ_p is varied between 0° and 360° while keeping the pump amplitude U_p and flow frequency f_a fixed.

Non-resonant parametric amplification can give selective gain or attenuation, depending on the pump frequency f_p and pump phase ϕ_p . Equal frequencies for flow and pump ($f_p = f_a$) give coherency in torque and spring softening, for which the pump phase determines whether the system will show relative amplification or attenuation. Therefore, it is

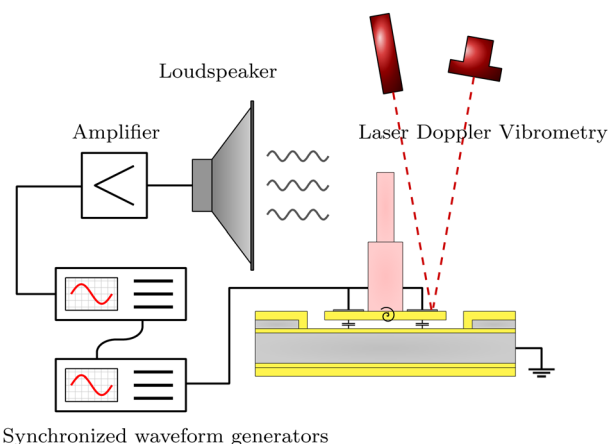


FIG. 3. (Color online) Measurement setup for determining the rotational angle of the hair flow sensor.

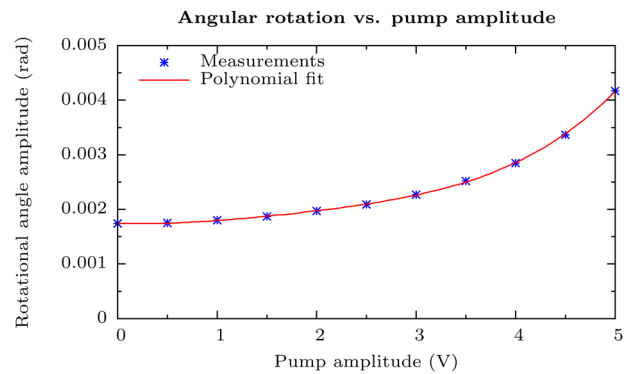


FIG. 4. (Color online) Amplitude of the periodic hair rotation angle as function of the pump amplitude U_p . The flow frequency f_a was equal to the pump frequency f_p (200 Hz), and the pump phase ϕ_p was set to the value giving maximum gain.

possible to realize a very sharp band pass/stop filter, depending on the pump settings.

Experiments were performed using the setup shown in Fig. 3. A waveform generator (Agilent 33220 A-001) is used to produce a sinusoidal signal at a frequency f_a that is supplied to an amplifier. This amplifier drives a loudspeaker (Visaton WS 17 E) to generate the harmonic air flow. A silicon wafer is glued onto the loudspeaker cone to achieve a flow profile that is well described by (very) near field theory.⁹ The AC-pump voltage supplied to the top electrodes is generated by a second waveform generator (Agilent 33220 A-001) that is synchronized with the first one to control the pump phase ϕ_p with respect to the air flow signal. The sensor rotational angle θ is derived from laser Doppler vibrometry using a Polytec MSA-400.

Experiments confirm that significant amplification of the sensor's response to the flow signal can be achieved for a suitable choice of pump parameters (Fig. 4). Here, the pump frequency f_p was set equal to the flow frequency f_a (200 Hz). The pump amplitude U_p was varied, and the phase ϕ_p was fixed at the value that produced maximum gain at $f_p = f_a$. A non-linear relationship between the rotational angle θ and the amplitude U_p of the applied pump voltage is observed, which is also expected by the quadratic nature of electrostatic actuation.

To investigate selective gain and filtering by PA, three frequencies were applied simultaneously to the loudspeaker

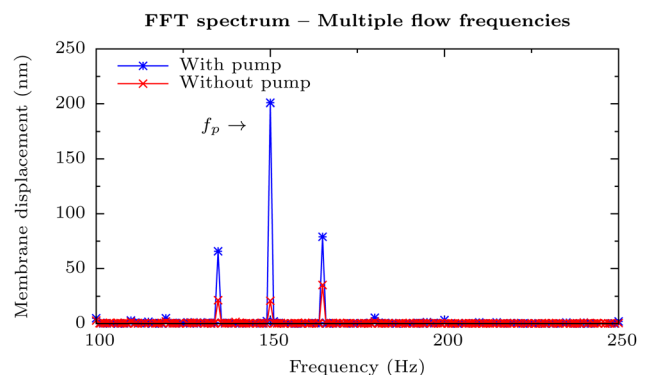


FIG. 5. (Color online) Measured gain of about 20 dB for the airflow frequency component at 150 Hz determined by FFT. The pump is fixed at $f_p = 150$ Hz with an amplitude of 5 V.

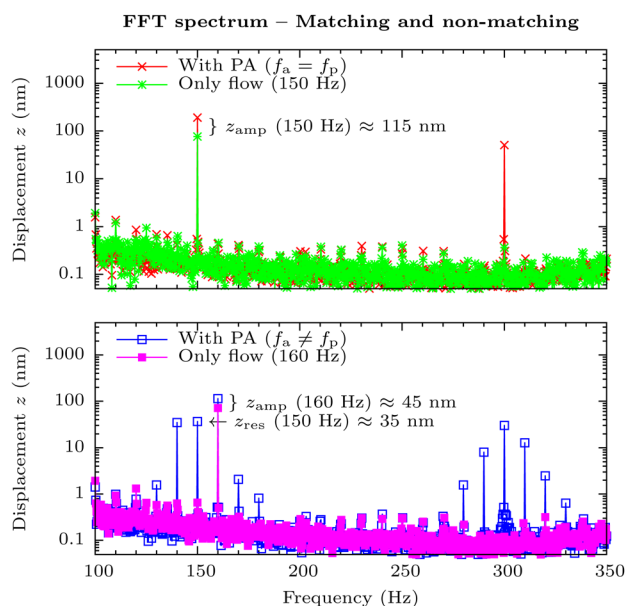


FIG. 6. (Color online) Amplitude spectrum for frequency matched (top) and mismatched (bottom) cases, with the pump fixed at 150 Hz, the phase value set to the value giving maximum amplification, and an amplitude of 5 V.

(using arbitrary waveform generation), resulting in a periodic air flow with three frequency components (135, 150, and 165 Hz). The pump frequency f_p was set to 150 Hz, with a pump amplitude U_p of 5 V. In Fig. 5, the spectrum of the hair rotational angle is shown for both the situations with and without pumping. Clearly, all three frequency components show gain, the maximum gain of about 20 dB experienced for the 150 Hz (matched) frequency. However, the ratio between the components changes when PA is applied to the system, resulting in a selective gain-advantage of 9 dB or more. This is in agreement with theory, which predicts frequency-independent amplification (135, 150, and 165 Hz) by the second term in Eq. (4) and frequency-dependent amplification (150 Hz) by the third term in Eq. (4), both for frequencies below resonance.

To determine mixing of frequencies and the residual membrane displacement z_{res} when using PA, the FFT amplitude spectra for both matching and non-matching flow and pump frequencies are examined (Fig. 6). For these measurements, the pump amplitude U_p is set to 5 V, the pump phase

ϕ_p was set to the value producing maximum gain, and the pump frequency f_p is fixed at 150 Hz. Then, the spectrum is measured both in the absence and presence of oscillating air flow (for cases $f_a = 150 \text{ Hz}$ and $f_a = 160 \text{ Hz}$). Similar to Fig. 5, by considering the increase in membrane displacement z_{amp} , selective gain is observed for matching frequencies (150 Hz, indicated by crosses, Fig. 6 (top)). For both cases with pump signal (crosses and open squares), the spectrum exhibits frequency components at and around twice the pump frequency ($2f_p = 300 \text{ Hz}$), as a result of vertical vibrations of the sensor's membrane (due to limited vertical stiffness and residual charges built-in the silicon-nitride layers) in combination with parametric mixing. Although there is a non-negligible contribution of the parametric pump at 150 Hz in the absence of a frequency matched flow (Fig. 6 (bottom), open square at 150 Hz), the gain achieved by pumping at the matched frequency (Fig. 6 (top), cross at 150 Hz) is significantly larger, confirming the applicability of parametric amplification for selective gain and filtering.

Concluding, non-resonant parametric amplification and filtering have been demonstrated in biomimetic hair-based flow sensors. By selecting appropriate values for the AC-pump voltage, selective gain and filtering are achieved. The responsivity to the incoming airflow can be improved by 20 dB, while having large selectivity with respect to non-matched frequency signals.

The authors would like to thank Vitaly Svetovoy for fruitful discussions. This work is carried out within the BioEARS-project, funded by STW/NWO.

- ¹D. Avitabile, M. Homer, A. R. Champneys, J. C. Jackson, and D. Robert, *J. R. Soc., Interface* **7**, 105 (2010).
- ²M. A. Dijkstra, J. J. J. van Baar, R. J. Wiegerink, T. S. J. Lammerink, J. H. de Boer, and G. J. M. Krijnen, *J. Micromech. Microeng.* **15**, S132 (2005).
- ³C. M. Bruinink, R. K. Jaganatharaja, M. J. de Boer, J. W. Berenschot, M. L. Kolster, T. S. J. Lammerink, R. J. Wiegerink, and G. J. M. Krijnen, in The 22nd IEEE International Conference on MEMS, Sorrento, Italy, 2009.
- ⁴D. Rugar and P. Grütter, *Phys. Rev. Lett.* **67**, 699 (1991).
- ⁵D. W. Carr, S. Evoy, L. Sekaric, H. G. Craighead, and J. M. Parpia, *Appl. Phys. Lett.* **77**, 1545 (2000).
- ⁶T. Shimozawa, T. Kumagai, and Y. Baba, *J. Comp. Physiol., A* **183**, 171 (1998).
- ⁷G. G. Stokes, *Trans. Cambridge Philos. Soc.* **9**, 8ff (1851).
- ⁸K. M. Harish, B. J. Gallacher, J. S. Burdess, and J. A. Neasham, *J. Micromech. Microeng.* **19**, 1 (2009).
- ⁹H. de Bree, V. Svetovoy, R. Raangs, and R. Visser, in The 11th International Congress on Sound and Vibration, St. Petersburg, Russia, 2004.